International Journal of Applied Engineering Research ISSN 0973-4562 Volume 13, Number 14 (2018) pp. 11428-11435

Design and Analysis of a Wideband Printed Monopole VHF Antenna for Airborne Applications

Mary Rani Abraham*, Sona O. Kundukulam

Naval Physical and Oceanographic laboratory,
Defense Research and Development Organization, Kochi, Kerala, India.

*(*Corresponding author)*

Abstract

Design and analysis of a novel wideband printed monopole antenna operating in VHF band has been presented for airborne applications. The antenna employs meandering technique as well as top loading technique for achieving compactness and wide band width. The substrate used for designing of antenna was FR4 Epoxy having a dielectric constant 4.4 and thickness 1.6mm. To evaluate the performance and characteristics with various dimensional parameters, a set of parametric analysis has been carried out. The variations in frequency domain response of the antenna has been explained, in terms of variations in distributed inductance and capacitance. The design equation for resonant frequency has been derived based on the parametric studies. Good agreement was achieved between the results calculated and those obtained by simulations using HFSS. The antenna exhibits a 3:1 VSWR bandwidth of 23%. The antenna has a size of $0.17\lambda_0$ X $0.14\lambda_0$ at lowest frequency of operation.

Keywords: Meander, printed monopole, VHF antenna, airborne.

INTRODUCTION

Modern aircrafts are sophisticated platforms with many antennas for communication, navigation and other purposes. The communicational and navigational antennas should have omnidirectional radiation pattern to provide wider coverage in the azimuthal direction. The limited space availability for antennas on aircraft demands antenna with wider bandwidth. Apart from these electrical constraints, airborne antennas should also meet certain mechanical requirements such as it should be light weighted, size compacted and aerodynamically designed.

Monopole antenna is simple, compact, lightweight and is easy to build in aerodynamic shape with minimum drag. Planar monopole antennas possess wide band characteristics along with omnidirectional radiation pattern. Owing to these qualities, they are the most preferred antennas for airborne applications [1].

Conventional airborne monopole antennas utilizes, the skin of airborne platform as its ground plane. The space constraints on the platform may result in insufficient ground plane for these antennas operating in HF/VHF band, which usually requires a ground plane of radius $\lambda/4$ at the lowest frequency of operation. The printed monopole antenna is a type of microstrip antenna that was modified into a printed form, where the radiator and ground plane were etched into the same plane reducing the mounting ground plane dependency of the conventional ones [2].

Meander line antenna is a potential candidate for miniaturized antenna with omnidirectional radiation pattern, with considerable radiation efficiency and negligible cross polarization. The planar meander antennas are constructed on dielectric substrate by continuously folding a conventional printed monopole patch. Meandering the patch increases the path over which the surface current flows and results in lowering the resonant frequency. Conventional meander line antennas exhibit a narrow bandwidth. There are some proposed methods in the literature [3-6] that may be used to broaden the bandwidth of these antennas.

In this paper, a novel printed monopole antenna has been presented, which uses meandering and top loading techniques to achieve low profile, wideband characteristics. A preliminary study of this antenna has been reported in [7]. Meandering and top loading are implemented on radiating patch as well as on ground patch to attain the wide bandwidth. Different parametric analysis were carried out to study performance characteristics of the structure with various dimensional parameters. Variations in frequency domain response of the antenna with dimensional parameters were explained by variations in distributed inductance and capacitance during analysis. The design equation for resonant frequency was derived from parametric studies and verified for various set of dimensional values. Good agreement has been achieved with calculated results and those obtained from HFSS simulations. The conferred antenna does not contain any external lumped elements or extra ground planes or matching circuits.

ANTENNA DESIGN

The substrate used for designing antenna was FR4 Epoxy having a dielectric constant (ε_r) 4.4 and thickness (h) 1.6 mm. Geometry of the proposed antenna is shown in Figure 1 with its dimensions listed in Table 1. The patch at top side of substrate was drawn in black and bottom in grey. The height of the antenna was 39 cm and substrate dimensions were 39 cm. X 31 cm. X 0.16 cm. A meander line monopole antenna with equal vertical and horizontal sections was employed symmetrically in the radiating patch and the ground plane. The length of each vertical and horizontal meander line was 2 cm. and the width was 0.5 cm. Edge feeding was used to excite the antenna with

port impedance 50Ω. The meandering and top loading at radiating patch generate one resonant frequency and the ground patch generate another resonant frequency. The parameters were optimized in such a way that the two resonances merge to form a wide band width.

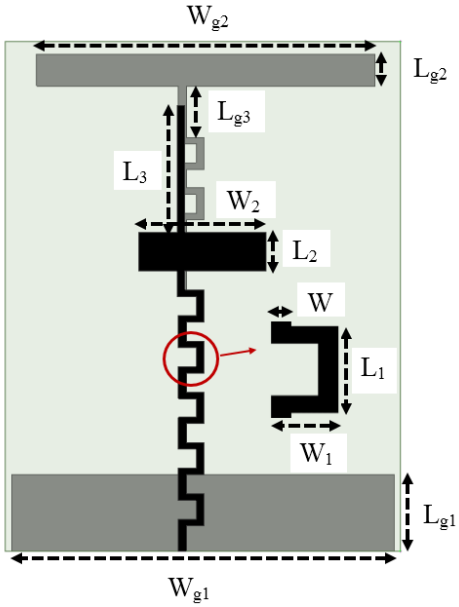

Figure 1. Geometry of proposed antenna

Table 1: Dimensions of the proposed antenna in cm.

L_1	2.0	**W_2**	6.0	**W_4**	0.6	**L_{g2}**	2.5
W_1	2.0	**L_3**	9.0	**L_{g1}**	6.0	**W_{g2}**	28
L_2	3.0	**W**	0.5	**W_{g1}**	30.0	**L_{g3}**	3.0

PARAMETRIC ANALYSIS

An elaborated parametric analysis was performed on the antenna to study about the influence of each parameter on the radiation characteristics. In order to explain variations in frequency domain response of the antenna, variations in distributed inductance and capacitance were also analyzed. All the dimensions were found to be critical and were optimized to get the optimum performance for a compact, low-profile wideband antenna in VHF band.

The extraction of distributed capacitance, inductance and resistance were executed by approximating the antenna to series RLC networks [8] with specific resonant frequency and Q factor. The distributed components corresponding to resonant frequency were extracted from reflection coefficient of the antenna. The resonant frequency and band width of the antenna were retrieved from reflection coefficient. The algorithms used for extraction of parameters are given below:

Step1: Calculate bandwidth **BW** and resonant frequency **Fr** from reflection co-efficient.

Step2: Calculate resistance **R** of circuit at resonance by solving equation

$\frac{R-Z0}{R+Z0} = \mathbf{10}^{(S_{11}/20)}$**;** where return loss was measured at resonant frequency and Z_0=50 Ω was the characteristic impedance of transmission line used to guide energy into the antenna.

Step3: Calculate Q by the relation **Q=Fr/BW.**

Step4: Calculate inductance L by the formula =**RQ/ 2πFr**.

Step5: Calculate capacitance C by the formula **C=1 / 2πQRFr**

Effect of ground plane dimensions

The effect of ground plane dimension L_{g1} was studied and is plotted in Figure 2(a). The variation in distributed parameters with variation in L_{g1} is plotted in Figure 2(b).

The bandwidth of the antenna was seen increasing on increase of L_{g1} from 2cm to 6cm, and on further increase of L_{g1} showed a decrease in the bandwidth of the antenna. This is due to the decrease in inductance and increase in capacitance as L_{g1} increases from 2 cm. to 6 cm. Further increase in L_{g1} decreases capacitance and bandwidth of the antenna decreases. Hence L_{g1}=6 cm was chosen as the optimum value.

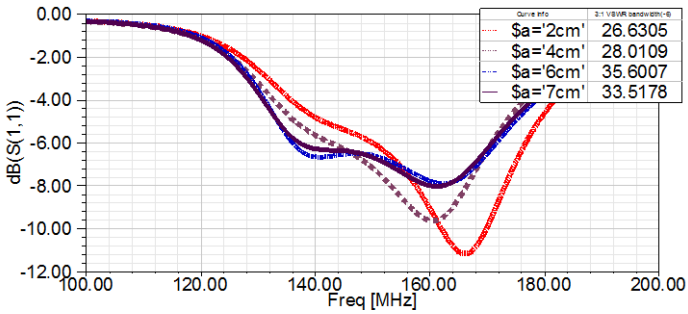

(a)

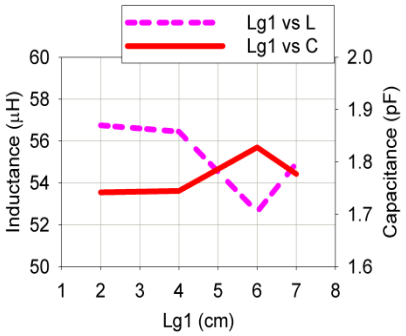

(b)

Figure 2. (a) Effect of L_{g1} on return loss of antenna. **(b)** Variation of reactive components with L_{g1}.

The effect of W_{g1} on frequency response of antenna was studied by varying it from 8 cm to 15 cm symmetrically to both sides from the center of antenna. As observed from Figure 3, W_{g1} is

a frequency determining factor. The increase in W_{g1} decreases resonant frequency. The impedance matching at 140 MHz improves on increase of W_{g1}, increasing bandwidth.

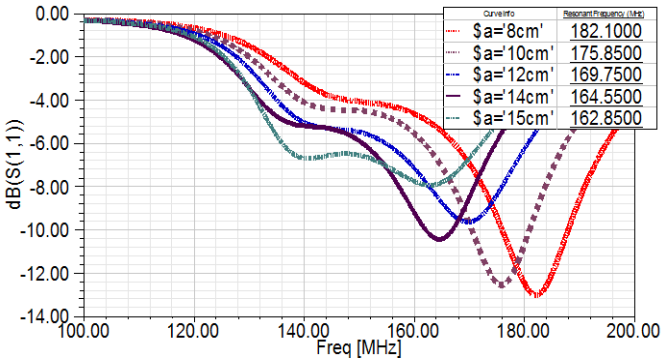

Figure 3. Effect of W_{g1} on return loss of antenna.

The frequency domain response of antenna with variations in W_{g2} was studied and is shown in Figure 5. It could be observed that, increase in W_{g2} from 7 cm to 14 cm symmetrically to both sides, leads to decreased resonant frequency.

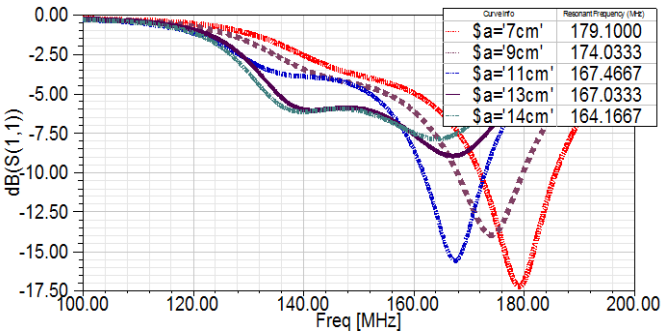

Figure 5. Effect of W_{g2} on the return loss of the antenna.

The effect of ground plane dimension L_{g2} was studied by varying it from 1 cm to 3 cm and is plotted in Figure 4 (a). It was found that as L_{g2} increases from 1 cm to 2.5 cm, the impedance matching at 140 MHz improves, increasing the bandwidth of antenna. It was evident from Figure 4(b) that increase in bandwidth is due to increase in distributed capacitance of antenna. Further increase in L_{g2} increases the inductive reactance, decreasing the bandwidth of antenna. Hence, L_{g2} = 2.5 cm was chosen as the optimum value.

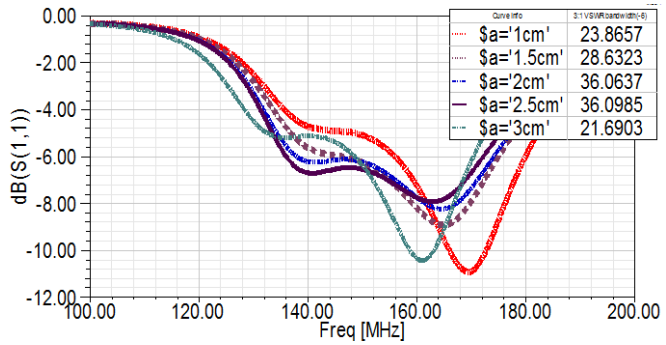

(a)

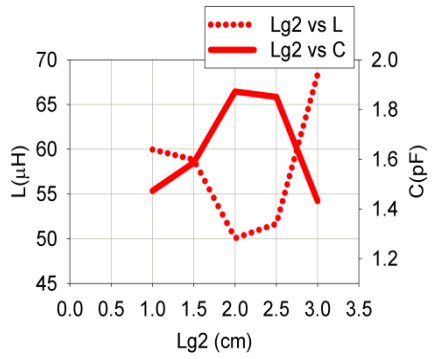

(b)

Figure 4. (a) Effect of L_{g2} on return loss of antenna.
(b) Variation of reactive components with L_{g2}.

Figure 6 (a) shows the frequency response of the antenna with variations in L_{g3}. As L_{g3} increases, the resonant frequency decreases. Also as L_{g3} is increased, the impedance matching at 140 MHz increases causing increase in bandwidth. The variations in the distributed parameters with variation in L_{g3} is shown in Figure 6 (b). The shift in resonant frequency was due to the predominance of variation in distributed inductance.

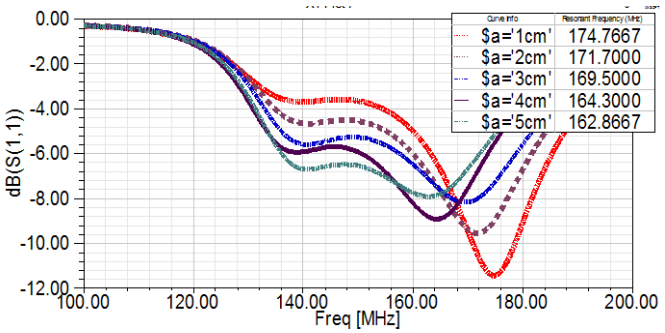

(a)

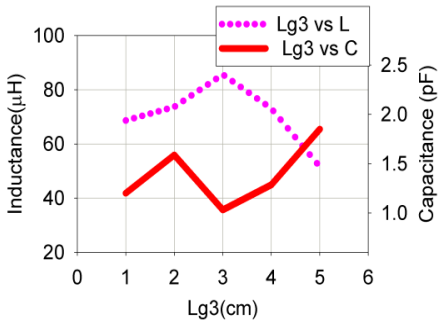

(b)

Figure 6 (a) Effect of L_{g3} on return loss of antenna.
(b) Variation of reactive components with L_{g3}.

Effect of radiating patch dimensions

The effect of L_2 was studied by varying it from 1 cm. to 4 cm and is plotted in Figure 7 (a). The variation in distributed parameters with L_2 is plotted in Figure 7(b). As L_2 increases from 1 cm to 4 cm, the impedance matching of the antenna improves till 3 cm and then decreases. The bandwidth of the antenna increases with increase in L_2 due to the increase in capacitive reactance. Further increase in L_2 decreases the capacitive reactance resulting in decreased bandwidth.

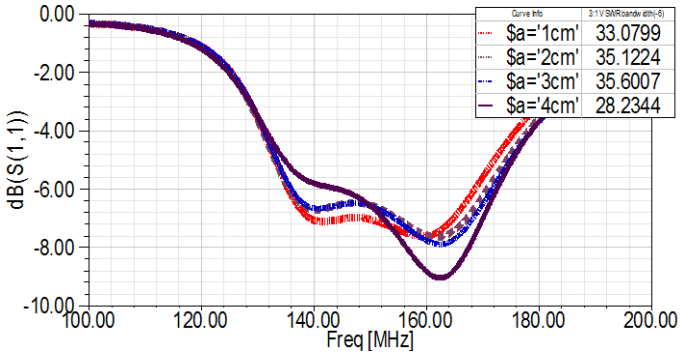

(a)

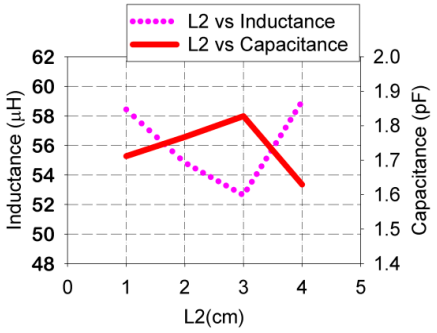

(b)

Figure 7 (a) Effect of L_2 on return loss of antenna.
(b) Variation of reactive components with L_2.

Figure 8 (a) shows the effect of variation of W_2 on return loss of the antenna and Figure 8 (b) plots the variation in distributed parameters with variation in W_2. As W_2 was increased symmetrically from 1 cm to 4 cm symmetrically to both sides, the impedance matching is improved till 3 cm and further increase cause decrease in impedance matching at 140 MHz The distributed capacitance increases as W_2 was increased from 1 cm. to 3 cm and cause increase in bandwidth. Further increase in W_2 caused a decrease in capacitive reactance and increase in inductive reactance, thereby decreasing bandwidth.

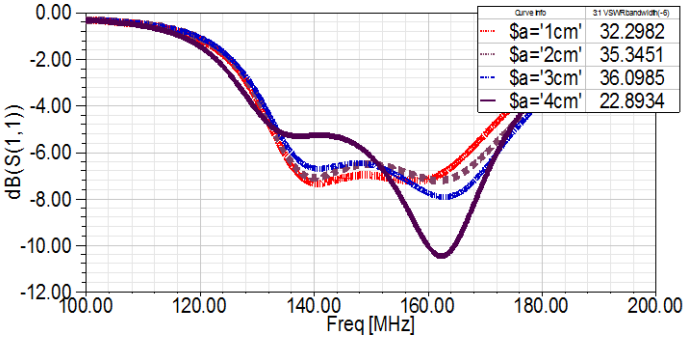

(a)

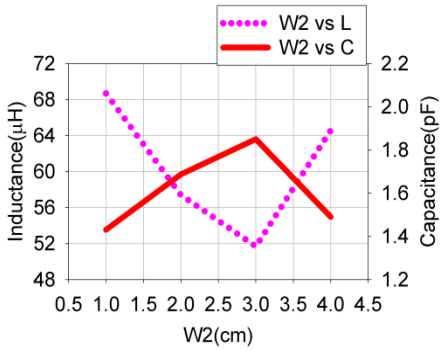

(b)

Figure 8 (a) Effect of W_2 on return loss of antenna.
(b) Variation of reactive components with W_2.

The effect of L_3 on frequency response of antenna is plotted in Figure 9 (a). As L_3 was varied from 1 cm to 12 cm, it could be observed that, there was a shift in the mode of resonance. A resonance near 140 MHz was observed as L_3 was 1 cm, which was due to the meandering and top loading patch at the ground plane. When this dimension was varied from 1 cm to 9 cm, it could be observed from the smith chart (Figure 9 (b)) that the impedance became more capacitive and the bandwidth is increased. At L_3 = 10 cm, a second resonance originated near 162 MHz and becomes dominant on further increase. This might mean that the coupling between the patch at the top and bottom played an important role in generating a resonance at 160 MHz L_3 = 11 cm was chosen as the optimum value as it has given maximum bandwidth.

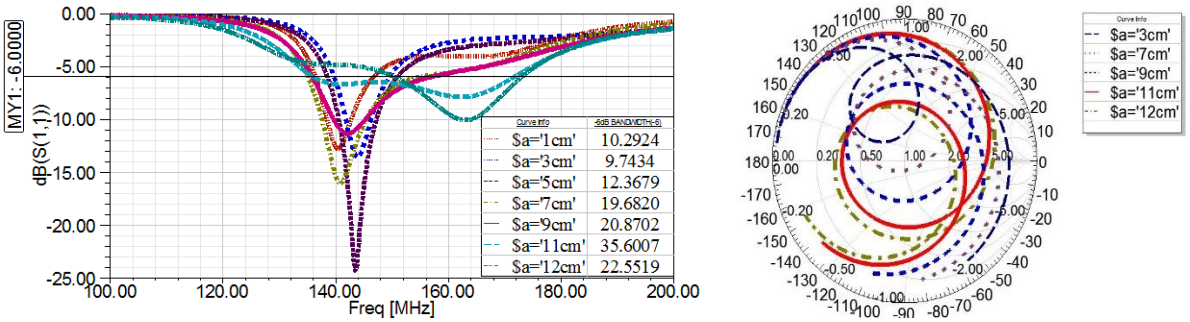

(a) **(b)**

Figure 9 (a) Effect of L3 on return loss of antenna.
(b) Input impedance loci of antenna for various values of L_3.

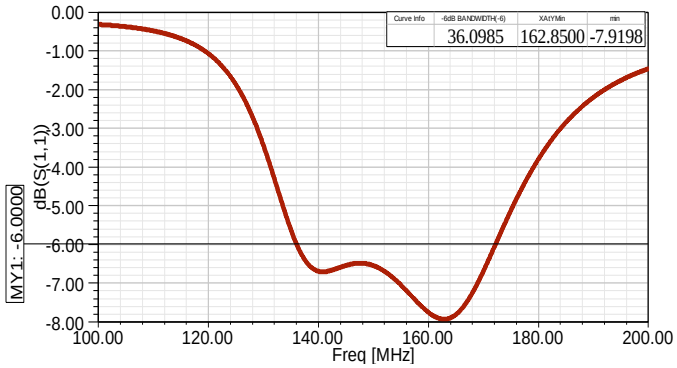

Figure 10. Reflection characteristics of Antenna.

RADIATION CHARACTERISITICS

The return loss characteristics of the antenna is plotted in Figure 10. The antenna showed a 3:1 VSWR bandwidth of 36 MHz. from 136 MHz. to 172 MHz.

The surface current distribution along radiating patch and ground plane is shown in Figure 11 (a) and (b) respectively. It could be observed that there was a λ/2 variation along the meanders of ground plane and radiating patch. The current distribution along top loadings were uniform, which contributed to increased radiation resistance of the antenna. The surface current distribution along adjacent horizontal portions of meanders had opposite phase. The transmission line current through horizontal segments has not contributed much to the radiated power or produced any losses.

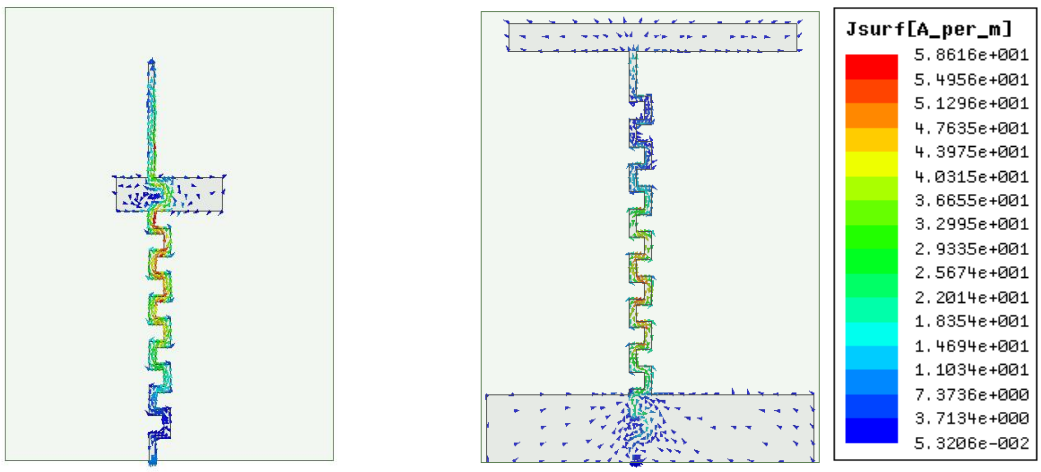

(a) (b)

Figure 11. Surface current distribution along. (a) Radiating patch, (b) Ground patch.

The E plane and H plane radiation pattern of the antenna at 140 MHz, 150 MHz, and 170 MHz are plotted in Figure 12 (a) and (b) respectively. The antenna showed an omnidirectional radiation pattern at all frequencies of the band. Simulations results also showed that the gain of the antenna was 1.75 dBi at the 170 MHz and 0.25 dBi at 136 MHz.

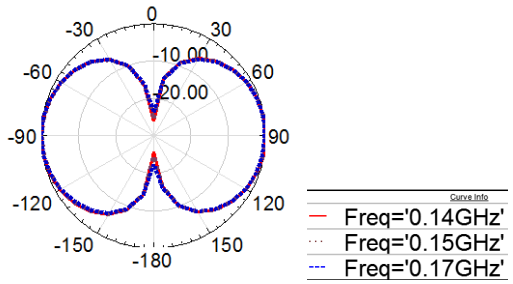

(a)

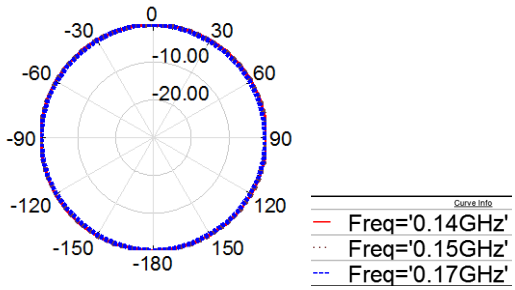

(b)

Figure 12. Radiation pattern of the antenna (a) E plane. (b) H plane.

DESIGN EQUATION

Design equation for meander monopole antenna was derived by Endo et.al [9]. The resonant frequency was decided by the physical dimensions of the meander lines, on the basis of height, width, number of folds and overall length of the meander structure. The resonant frequency of meander line monopole antenna composed of flat conductors was calculated using the formula:

$$N = \frac{\frac{\lambda}{4}(\log\frac{2\lambda}{b}-1)-(\log\frac{8l}{b}-1)}{w\log\frac{2l}{Nb}} \qquad (1)$$

Where ***w*** is antenna width, ***l*** is length of meander elements, ***b*** is conductor diameter and ***N*** is the number of turns.

To verify the concordance of this design equation in the proposed design, the antenna was simulated with only meander segments (Figure 13 (a)). The orange colour represents the ground patch at the bottom of substrate and the grey colour represents the radiating patch at the top. The return loss plot of this configuration is given in Figure 13 (b). The antenna showed 2 resonances – at 196 MHz, and 305 MHz The resonance at 305 MHz was due to the radiation from the top patch and at 196 MHz was due to the bottom patch.

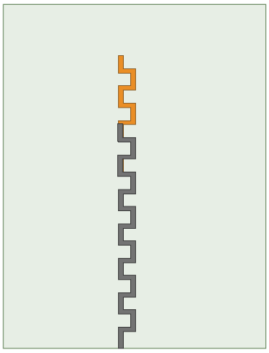

(a)

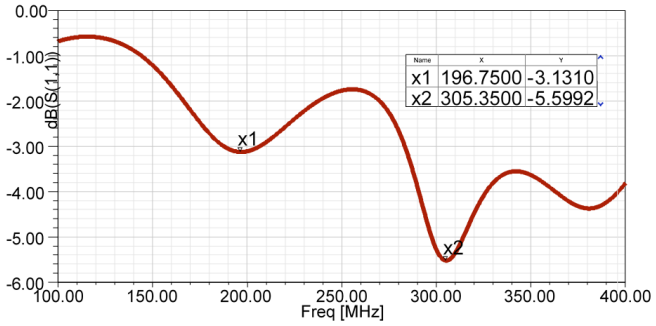

(b)

Figure 13 (a) Antenna with only meander segments. **(b)** Return loss plot of antenna with only meander segments.

Rearranging equation (1),

$$\left(\frac{2\lambda}{b}\right)^{\lambda/4} - e^{\lambda/4} = \left(\frac{8l}{b}\right)^{l} + \left(\frac{2l}{Nb}\right)^{Nw} - e^{l} \qquad (2)$$

The first resonance (λ = 153 cm) was evaluated by substituting the values of the meander line on the bottom patch: l = 34 cm, N = 16, w = 2 cm, b = 0.5 cm. The left side of (2) gave 10.194 while the right side gave the value 9.9. When considering the patch at the top of the substrate, the total length of meander line was 28 cm and number of turns was 12. The left side of (2) when evaluated for second resonance (λ = 98 cm) gave 3.04 whereas the right side of (2) gave the value 3.33. Thus the design equation proposed by Endo et.al has satisfied approximately for the meander segments of this antenna.

The relationship between the resonant frequency of meander line antenna and the geometrical parameters was proposed by BONNETT et.al [10] and was given by:

$$L_n(F_0) = a + bW_a + CN + dL + eW + f(N*W_a) + g(L*W_a) + h(W*W_a) + i(L*N) + j(N*W) + k(L*W) + lW_a^2 + mN^2 + oW^2 \qquad (3)$$

Where, W_a is the length of horizontal line of meander segment, ***L*** is the total length of antenna, ***W*** is the line width, ***N*** is the number of meander line. The pitch of the meander line was not used in this formulation of design equation as it depends up on

other factors. The current distribution along the meander line of the top patch showed a λ/2 variation at 305 MHz and ground patch showed a λ/2 variation at 196 MHz.

Considering equation (3) for the antenna configuration figure 13 (a), the variables were found as:

a=0.25; b=0.17; c=0.005; d=0.004; e=0.0045; f=0.0002; g= 0.002; h=0.0025; i=0.0024; j=0.025; k=0.0028; l=0.0002; m=0.0015; n=0.0018; o=0.005

Apart from length and number of meandering segments, the ground plane dimensions W_{g1}, W_{g2}, L_{g3} and radiating patch dimension L_3 determines the resonant frequency.

The design equation proposed for meandered top loaded printed monopole antenna is

$$L_f = 2*((0.4*W_{g1}) + (0.4*W_{g2}) + (0.3*L_{g3})) + L_{n1} + (0.2*L_3) + L_{n2} \quad (4)$$

Resonant frequency, $F = C/L_f$ (5)

For examining the validity of these conclusions, the antenna was designed for various values of W_{g1} W_{g2} and L_{g3} and simulated using HFSS software. In order to establish the influence brought by each parameter, the following methodology was used. First, two of the values were fixed and then, the unfixed one was changed over a range.

The comparison between the resonant frequencies derived from equation (5) and simulated using HFSS for various values of W_{g1}, W_{g2} and L_{g3} are shown in Figure 14. (a), (b) and (c) respectively. All in all, the resonant characteristics of meandered top loaded printed monopole antenna predicted by (5) has a general agreement with simulation results.

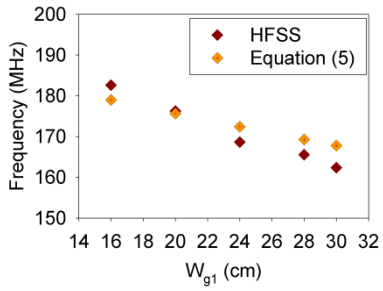

(a)

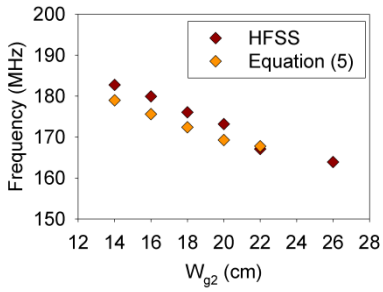

(b)

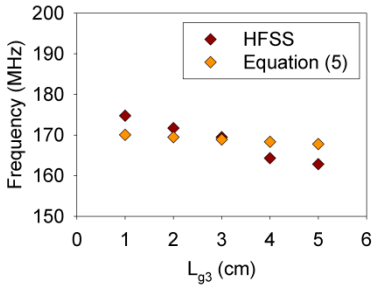

(c)

Figure 14. Variation in resonant frequency with (a) Wg1, (b) Wg2 (c) Lg3.

CONCLUSION

A compact wideband printed monopole antenna operating in VHF band was designed and the results are presented. A detailed parametric study was carried out and the effect of each dimension on antenna's radiation characteristics were analyzed. A design equation was proposed and validated for various set of dimensions. The stipulated equation involved all the geometrical parameters of the antenna.

REFERENCES

[1]. C. Sairam, T. Khumanthem, S. D. Ahirwar, and A. Kumar, "Design and development of broadband blade monopole antenna," in Proceedings of the International Conference of Recent Advances in Microwave Theory and Applications (MICROWAVE '08), pp. 150–151, Jaipur, India, November 2008.

[2]. J. Michael Johnson and Yahya Rahmat-Samii "The tab monopole", IEEE Transactions on Antennas and Propagation, Vol. 45, No. 1, pp 187-188, January 1997

[3]. Ju, D. K., T. H. Oh, J. M. Woo, and S. Y. Hong, "Double rectangular meander line loop monopole antenna for miniaturisation and bandwidth," Electronics Letters, Vol. 43, No. 16, 846–848, 2007.

[4]. Jung, J., H. Lee, and Y. Lim, "Modified meander line monopole antenna for broadband operation," Electronics Letters, Vol. 43, No. 22, 2007.

[5]. Noguchi, K., M. Mizusawa, T. Yamaguchi, and Y. Okumura, "Increasing the bandwidth of a meander line antenna consisting of two strips," in IEEE 1997 Digest Antennas and Propagation Society International Symposium, 2198–2201, 1997.

[6]. Jun Fan, Zhenya Lei , Yongjun Xie, and Mingyuan Man "Bandwidth Enhancement for Low Frequency Meander Line Antenna" Progress In Electromagnetics Research C, Vol. 51, 169–177, 2014.

[7]. Mary Rani Abraham and Sona O. Kundukulam, Wideband Printed Monopole VHF Antenna, 2015

International Conference on Computing and Network Communications (CoCoNet'15), Dec 16-19, 2015, Trivandrum, India.

[8] Bakshi, Uday A., and Ajay V. Bakshi. Antenna and wave propagation. Technical Publications, 2009.

[9]. Endo, T., Sunahara, Y. , Satoh, S. and Katagi, T. (2000), Resonant frequency and radiation efficiency of meander line antennas. Electron. Comm. Jpn. Pt. II, 83: 52-58.

[10]. Bonnet, Benoît, Fabrice Guitton, Yves Raingeaud, and Didier Magnon. "Resonant frequency, bandwidth and gain of meander line antenna." In Antenna Technology and Applied Electromagnetics [ANTEM 2005], 11th International Symposium on, pp. 1-4. IEEE, 2005.